Interactions between Ligand-Bound EGFR and VEGFR2

Michael D. Paul and Kalina Hristova *

Department of Materials Science and Engineering, *Institute for NanoBioTechnology, and Program in Molecular Biophysics, Johns Hopkins University, Baltimore, MD 21218, United States*

Correspondence to Kalina Hristova: *kh@jhu.edu (K. Hristova)*
https://doi.org/10.1016/j.jmb.2021.167006
Edited by Igor Stagljar

Abstract

In this work, we put forward the provocative hypothesis that the active, ligand-bound RTK dimers from unrelated subfamilies can associate into heterooligomers with novel signaling properties. This hypothesis is based on a quantitative FRET study that monitors the interactions between EGFR and VEGFR2 in the plasma membrane of live cells in the absence of ligand, in the presence of either EGF or VEGF, and in the presence of both ligands. We show that direct interactions occur between EGFR and VEGFR2 in the absence of ligand and in the presence of the two cognate ligands. However, there are not significant heterointeractions between EGFR and VEGFR2 when only one of the ligands is present. Since RTK dimers and RTK oligomers are believed to signal differently, this finding suggests a novel mechanism for signal diversification.

The 58 Receptor Tyrosine Kinases (RTKs) sense the extracellular environment and initiate cellular responses such as growth, survival, differentiation, and motility.[1,2] They are single-pass membrane proteins with extracellular (EC) N-terminal ligand-binding domains and intracellular (IC) regions containing the kinase domains. RTKs respond to extracellular ligands by associating into ligand-bound dimers or, sometimes, higher-order oligomers.[3–5] Dimerization brings the kinase domains into close proximity, so they can cross-phosphorylate and activate each other. Phosphorylated tyrosines in the IC domain serve as docking sites for cytoplasmic effector proteins, which trigger the downstream signaling cascades that control cell fate.[6,7] All RTKs are critically important for normal physiological processes, and are implicated in many diseases.[8–10] Despite decades of research, however, many aspects of RTK activation are not well understood, and this lack of knowledge is an impediment to the development of effective and specific therapies.

Typically, investigations have focused on specific RTKs, in efforts to define the role of each RTK in cell physiology and in disease. In addition, there has been interest in uncovering common principles and in developing mechanistic models of RTK activation. After the discovery of RTKs in the 1970s, a simple model of RTK activation was proposed: the ligands act as cross-linkers to induce RTK dimerization.[11,12] This "canonical" model, however, cannot explain all experimental observations in the literature.[13,14] Instead, most observations can be explained within the context of the more complex "transition model" of RTK activation.[15] The transition model states that (1) RTKs have a propensity to interact laterally and to form dimers even in the absence of ligand, (2) different unliganded RTK dimers have different stabilities, (3) ligand binding leads to RTK dimer stabilization or oligomerization, and (4) ligand binding induces structural changes in the RTK dimer.

Within the framework of the transition model, the ligand plays two roles: it stabilizes RTK dimers and oligomers and induces a structural change in the receptors.[15] Details about the structural changes due to ligand binding have been elusive, as there are no high resolution full-length RTK structures. Nevertheless, many biochemical and biophysical experiments, albeit indirect, are consistent with the idea of ligand-induced structural changes.[16–21] Furthermore, addition of ligand leads to a substantial increases in RTK phosphorylation and in downstream signaling, but typically induces only a modest increase in RTK interactions.[18,19,22,23] Thus, there is strong support for the idea that unliganded and ligand-bound RTK dimers/oligomers have different stabilities, structures, and activities. As such, they are viewed as different signaling entities within the context of the transition model.[15]

Most cell types express multiple RTKs, and these RTKs can also engage in heterointeractions, in addition to homointeractions.[24] Heterointeractions are easily incorporated into the transition model, which can explicitly account for all relevant interactions with the help of thermodynamic cycles.[15] The extent of the different heterointeractions in the transition model is determined by the relative expression levels of the interaction partners, in accordance with the law of mass action.[24]

It has long been recognized that RTKs that belong to the same subfamily (a group of receptors with homologous EC domains) can engage in heterointeractions.[24] First, common ligands were proposed to drive these interactions, but now it is clear that heterointeractions can occur in the absence of a common ligand, and even in the absence of any ligand.[25–28] More recent work has demonstrated that RTKs engage in heterointeractions not only within subfamilies, but also across the 20 different subfamilies; the literature of this subject was reviewed in detail recently.[24] To gain insights into these processes, we recently used quantitative fluorescence microscopy to study the heterointeractions of nine unrelated RTK pairs in the plasma membrane, in the absence of ligand.[29] We showed that these RTKs can form unliganded heterodimers which, surprisingly, were almost as stable as the respective unliganded homodimers.[29] We further showed that the abundance of the homo- and heterodimers is regulated by ligand binding. In particular, the addition of a cognate ligand abolished the heterodimer population, likely as a consequence of homodimer stabilization due to ligand binding.[29]

While the depletion of heterodimers upon ligand binding can be predicted by the law of mass action, this depletion appears largely inconsistent with a large body of literature which documents significant biological effects due to heterodimerization in the presence of ligands.[24] For example, endogenous FGFR1, FGFR2, and FGFR3 appear to interact with endogenous EphA4 in neuronal cells only in the presence of the ligand ephrin-A1.[30] Significant interactions between ROR1 and EGFR have been detected in the presence of the ligand EGF, in lung carcinoma cells that endogenously express both receptors.[31] ROR1 interacts with ErbB3 in triple negative breast cancer cells in the presence of the ligand neuregulin-1, resulting in ErbB3 phosphorylation on a unique tyrosine, Tyr1307.[32] Other examples include TrkA-ErbB2 heterointeractions in the presence of the ligand NGF;[33] TrkB-ErbB2 interactions in response to the ligand BDNF, resulting in increased ErbB2 phosphorylation;[34] and MET-VEGFR2 interactions in the presence of the ligand HGF, leading to MET phosphorylation.[35] Of particular note, PDGFRβ and VEGFR2 were found to coimmunoprecipitate in the presence of both VEGFA and PDGF-BB, but not when only one or neither ligand was present,[36,37] suggesting that both cognate ligands may be necessary for some heterointeractions. A question therefore arises whether direct heterointeractions may occur between ligand-bound receptors from unrelated RTK subfamilies. Thus far, insights have come almost exclusively from co-immunoprecipitation experiments,[24] but this possibility has not been investigated using direct quantitative biophysical methods. However, such heterointeractions could have significant biological implications, as they involve receptors that are in their highly active liganded configurations.[4,38–40]

One pair of receptors that has been shown to engage in direct heterointeractions is the pair of EGFR and VEGFR2. The interactions between these two receptors are of interest, because they are often co-expressed in cells and because of substantial crosstalk between the two signaling pathways.[41–43] Furthermore, the activity of one receptor can interfere with cancer treatments that seek to inhibit the other receptor.[44–46] Here, we test the hypothesis that these two receptors interact directly in the plasma membrane when they are ligand-bound. To directly detect heterointeractions between EGFR and VEGFR2 in the plasma membrane, we performed hetero-FRET experiments in which one of the RTKs was labeled with mTurquoise (MT, a FRET donor) and the other with YFP, a FRET acceptor. Because of the labeling scheme used, the detection of FRET in this experiment is a direct demonstration of the presence of heterointeractions.

Previously, we have studied these interactions in the absence of ligand.[29] As both full-length EGFR and full-length VEGFR2 exhibited poor expression in HEK 293 T cells,[29] the most informative experiments utilized versions of the receptors that contained the entire EC and transmembrane (TM) domains, while the IC domains were replaced with the fluorescent protein reporters. We found that

these versions, referred to as "ECTM EGFR" and "ECTM VEGFR2," directly interact in the absence of ligand. Importantly, these interactions occurred even when the intracellular domains, known to contribute stabilizing contacts within RTK dimers, were not present, suggesting that the interactions are significant. This conclusion was supported by further data analysis, which revealed that ECTM EGFR and ECTM VEGFR2 form a heterodimer with stability that is similar to the stabilities of the ECTM EGFR and ECTM VEGFR2 unliganded homodimers.[29]

The FRET measurements followed a quantitative protocol (termed FSI-FRET)[47] which yields (i) the donor concentration, (ii) the acceptor concentration, and (iii) the FRET efficiencies in the plasma membrane of individual cells.[47] Because transient expression levels vary from cell to cell, a wide range of receptors concentrations were sampled and measured in each transfection experiment. A few hundred cells, imaged across multiple independent experiments, were analyzed, and the data were combined.

Spectral images were acquired under two-photon excitation using a Mai Tai femtosecond mode-locked laser (Spectra Physics), the OptiMiS True Line Spectral Imaging system (Aurora Spectral Technologies), and a Zeiss Observer wide field microscope with a 63X NA 1.2 water immersion objective as described.[48] Two scans were performed: a "FRET scan" with excitation at $\lambda_1 = 840$ nm, in which the donor is maximally excited and an "acceptor scan" with excitation at $\lambda_2 = 960$ nm, in which the acceptor is maximally excited.[47] The output of these scans were a set of complete spectra in each pixel of the plasma membrane.

Figure 1 shows pixel-level emission spectra of ECTM EGFR-MT and ECTM VEGFR2-YFP, expressed in HEK 293 T cells, acquired at $\lambda_1 = 840$nm and $\lambda_2 = 960$nm (FRET and acceptor scan, respectively). These spectra are then unmixed into donor and acceptor components as described.[47] To accomplish this, cells in control experiments were transfected with a single receptor, to acquire emission spectra of the donor only and the acceptor only, to serve as a basis for the unmixing. Pixel-level control spectra were averaged over many pixels and smoothed over the emission wavelengths[26] to produce the basis spectra F^D_{basis} for the donor and F^A_{basis} for the acceptor. Then, the hetero-FRET emission spectra, $F(\lambda)^{pixel}_{\lambda_1,\lambda_2}$, as the ones in Figure 1, are assumed to be a linear sum of three contributions: the fluorescence of the donor in the presence of the acceptor, $F^{DA}(\lambda)$, (with the spectral features of F^D_{basis}); the fluorescence of the acceptor in the presence of the donor, $F^{AD}(\lambda)$ (with the spectral features of F^A_{basis}); and a background contribution (see Figure 1). The unmixing of $F(\lambda)^{pixel}_{\lambda_1,\lambda_2}$ per each pixel was performed using linear least squares optimization in MATLAB, as described in detail in King *et al.*[47] The unmixed spectra are then integrated to yield the cumulative fluorescence intensities.

To calculate concentrations from the integrated fluorescence intensities, we also imaged solution standards of the donor and acceptor fluorophores. Four known concentrations of soluble fluorescent proteins were imaged at both excitation wavelengths, and a line of slope *i* was fit to the integrated intensity *versus* concentration data for every pixel of the image.[47] The four slopes, $i_{D,\lambda1}$, $i_{D,\lambda2}$, $i_{A,\lambda1}$, and $i_{D,\lambda2}$, were calculated for every pixel, for both the donor and acceptor solution standards, at the two excitation wavelengths,λ_1 and λ_2. As shown previously,[47] the fluorescence properties of the fluorescent proteins are the same in cells and in the calibrating solutions, which allows a direct comparison.

From these experiments, we calculated (i) the donor concentration [D], (ii) the acceptor

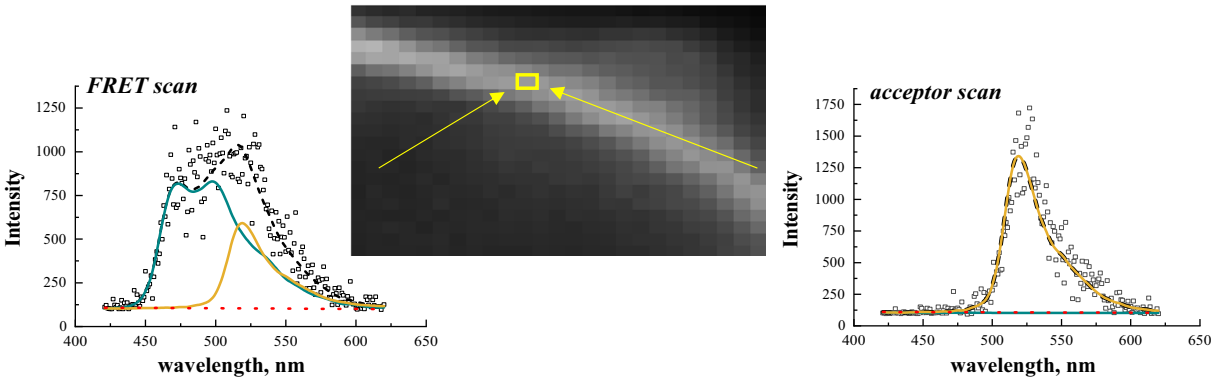

Figure 1. Examples of a FRET and acceptor spectra, acquired in a single pixel in the plasma membrane (highlighted in yellow), for the FRET pair of MT and YFP. The FRET spectrum is acquired at the excitation wavelength of 840 nm in a two photon microscope, and the acceptor spectrum is acquired at the excitation wavelength of 960 nm. Each single pixel fluorescence spectrum (open black symbols) is decomposed as a linear sum (black dashed line) of the donor (turquoise line), acceptor (yellow line), and background (dotted red line) contributions.

concentration [A], and (iii) the FRET efficiencies in the plasma membrane of each individual cell using the following equations:

$$FRET = 1 - F^{DA}_{\lambda 1}/F^{D}_{\lambda 1} \quad (1)$$

$$[D] = \frac{F^{D}_{\lambda 1}}{i_{D,\lambda 1}} = F^{DA}_{\lambda 1}\frac{1}{i_{D,\lambda 1}} + \frac{Q^{D}}{Q^{A}}\left(F^{AD}_{\lambda 1} - \frac{i_{A,\lambda 1}}{i_{A,\lambda 2}}F^{A}_{\lambda 2}\right)) \quad (2)$$

$$[A] = \frac{F^{A}_{\lambda 2}}{i_{A,\lambda 2}} = \frac{1}{i_{A,\lambda 2}}\left(F^{AD}_{\lambda 2} - \frac{i_{D,\lambda 2}}{i_{D,\lambda 1}}F^{AD}_{\lambda 1}\right)\cdot\left(1 - \frac{i_{A,\lambda 1}}{i_{A,\lambda 2}}\frac{i_{D,\lambda 2}}{i_{D,\lambda 1}}\right)^{-1} \quad (3)$$

In these equations, *FRET* is the measured FRET efficiency. $F^{D,A}_{\lambda 1,2}$ is the total fluorescence of the donor or acceptor in the absence of FRET for excitation at λ_1 or λ_2. $F^{DA}_{\lambda 1}$ is the measured (quenched) fluorescence of the donor in the presence of acceptors, and $F^{AD}_{\lambda 2}$ is the measured fluorescence of the acceptor, enhanced due to FRET. $i_{D,\lambda 1}$ and $i_{A,\lambda 2}$ are the slopes of the solution standard intensity *versus* micromolar concentration curves. Q_A and Q_D are the quantum yields of the donor and the acceptor.

To report [A] and [D] as 2D concentrations, the pixel-level fluorescence intensities for F^D, F^A, and F^{AD} are integrated (summed) over a membrane region (reg). The total integrated fluorescence of the region, $F^{DA}_{\lambda 1,reg}$, $F^{D}_{\lambda 1,reg}$, or $F^{A}_{\lambda 2,reg}$, is then divided by the arc length of the region to calculate the average integrated fluorescence per unit length of membrane. To obtain the effective 2D concentration from the 3D concentration, the mean integrated fluorescence is multiplied by the pixel width as described in detail in King *et al.*[47]

The black symbols in Figure 2 show the hetero-FRET between ECTM-EGFR and ECTM-VEGFR2 in individual cells, in the absence of ligand.[29] The solid black line in all panels is the so-called proximity FRET,[49,50] which occurs when a donor and an acceptor are randomly close to each other in the absence of specific interactions.[49,50] The shown dependence of proximity FRET on acceptor concentration, derived mathematically,[49,50] has been verified experimentally using LAT as a monomer control in prior work[29]; the LAT data are shown as green symbols in all panels of Figure 2.

The hetero-FRET data measured for ECTM EGFR and ECTM VEGFR2 in the absence of ligand (black symbols in all panels) lie above the proximity line, indicative of specific hetero-interactions. However, we previously found that the addition of 10 nM EGF (effectively saturating concentration, since the effective EGF-EGFR dissociation constant is ~1 nM[51]) decreased the FRET efficiencies to the point that the hetero-FRET straddled the proximity FRET line (red symbols in Figure 2(B)). This is an indication that heterointeractions are abolished in the presence of EGF.[29]

To test the hypothesis that interactions can also occur between ligand-bound EGFR and ligand-bound VEGFR2, we performed hetero-FRET experiments in the presence of both EGF and VEGF. Both ligands were added at high concentrations: 10 nM for EGF (as in Figure 2(B)) and 56 nM for VEGF. Effective dissociation constants for VEGF binding to VEGFR2 are in the range 75 pM to a few nM,[52–55] and thus this experimental design ensures that the vast majority of the receptors are ligand-bound. The measured hetero-FRET efficiencies in individual cells, which report on the heterointeractions between ligand-bound receptors, are shown in Figure 2(C) with the purple symbols. Most hetero-FRET efficiencies now appear above the FRET proximity line, thus revealing heterointeractions in response to the two ligands.

In control experiments, we added 56 nM VEGF (but no EGF) and we measured the hetero-FRET between ECTM EGFR and ECTM VEGFR2. The measured hetero-FRET *versus* acceptor concentration is shown in Figure 2(D) with the pink symbols. The hetero-FRET now straddles the monomer proximity FRET, similar to what occurred after the addition of EGF. This indicates a significant decrease in the heterointeractions when only VEGF is present, as compared to the case when both ligands are present.

To obtain a quantitative measure of the deviation of the measured hetero-FRET from proximity FRET, we subtracted the proximity FRET from the experimental measurements. Histograms of the deviations from proximity FRET in the individual cells are shown in Figure 3(A)–(E). The averages and the standard errors are compared in Figure 3(F). We see that the deviation from proximity is not statistically significant in the presence of either EGF or VEGF, but is highly significant when the two ligands are present. Thus, one ligand is insufficient for heterointeractions between EGFR and VEFR2; instead both ligands are required. These results suggest that the observed FRET is due to interactions between ligand-bound EGFR and ligand-bound VEGFR2.

Taken together, the data show that ECTM EGFR and ECTM VEGFR2 engage in direct interactions in the plasma membrane, in the absence of ligand and in the presence of the two cognate ligands, EGF and VEGF. However, there are no significant heterointeractions between ECTM EGFR and ECTM VEGFR2 when only one of the cognate ligands is present.

This interesting observation can be explained by the idea that unliganded EGFR and VEGFR2 interact in the plasma membrane, and so do ligand-bound EGFR and VEGFR2. On the other hand, unliganded VEGFR2 and liganded EGFR do not interact significantly, and neither do unliganded EGFR and liganded VEGFR2. This is a fundamentally novel observation, which is straight-forward to interpret in the context of the transition model of RTK activation, since the

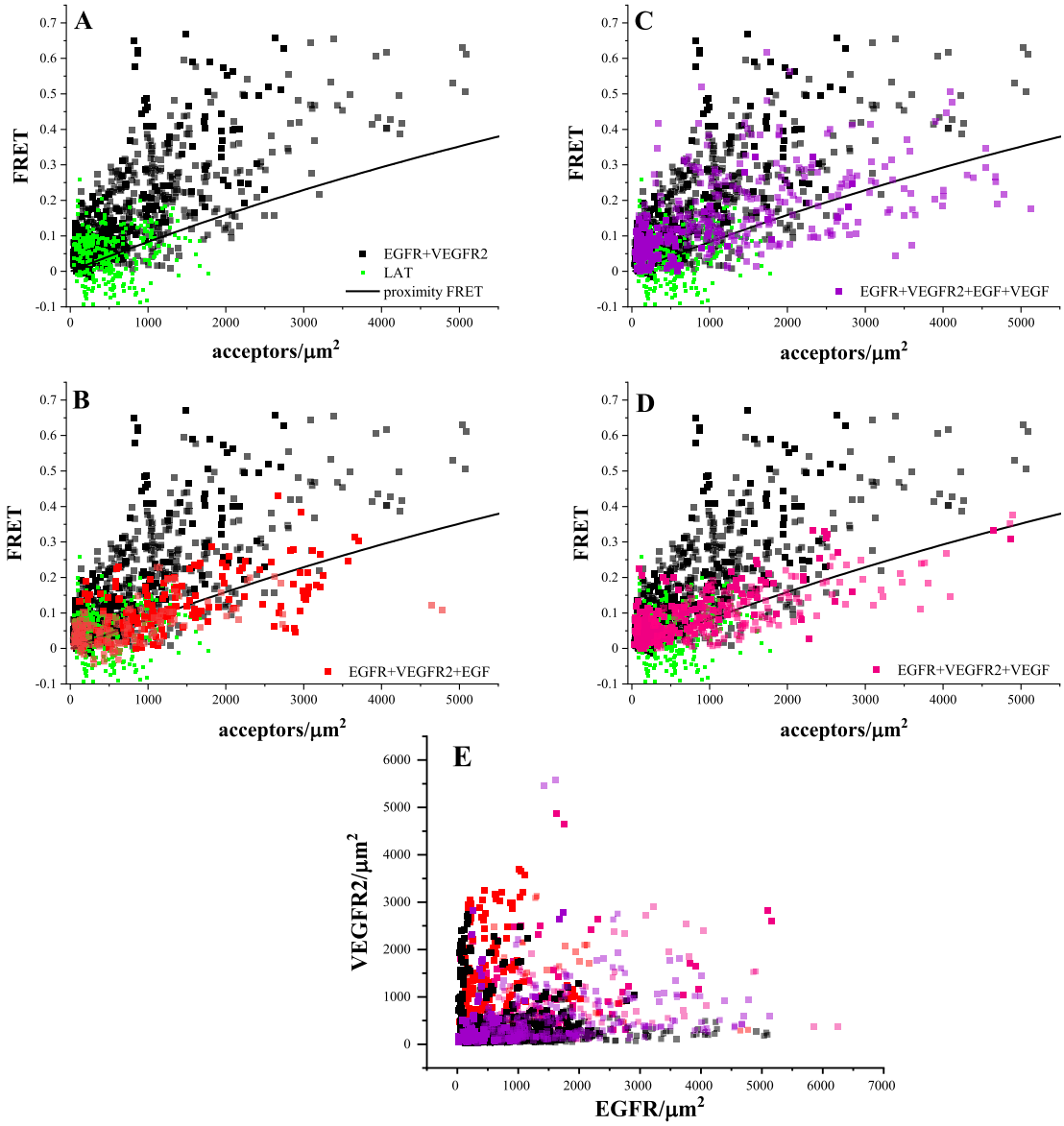

Figure 2. Hetero-FRET *versus* acceptor concentrations. Hetero-FRET efficiencies are measured in ~2–3 μm stretches of plasma membrane of live HEK 293 T cells, using the FSI-FRET method,[47] and are plotted as a function of acceptor concentration. The solid black line shows the proximity FRET, which accounts for the random close approach of donor and acceptor in the membrane. This is the highest FRET that can occur in the absence of specific receptor interactions. As discussed previously,[49,50] it depends mainly on the acceptor concentration. The protein LAT (green) is used as a negative control as it is known to be monomeric[63–65]; FRET data for LAT straddle the FRET proximity line.[29] Black symbols show the measured FRET for EGFR-VEGFR2 heterodimerization in the absence of ligand,[29] in cells that were co-transfected with varying ratios of ECTM EGFR and ECTM VEGFR2, with a total of 0.5–4 μg of ECTM EGFR DNA and 3–6 μg of ECTM VEGFR2 DNA. Solid black symbols correspond to FRET experiments where VEGFR2 was labeled with the acceptor, YFP, and transparent black symbols correspond to FRET experiments where EGFR was labeled with YFP (844 data points total). (B) Effect of 10 nM EGF on EGFR-VEGFR2 hetero-FRET.[29] Solid red symbols correspond to FRET experiments where VEGFR2 was labeled with YFP, and transparent red symbols correspond to FRET experiments where EGFR was labeled with YFP (302 data points total). (C) Effect of 10 nM EGF and 56 nM VEGF on EGFR-VEGFR2 hetero-FRET. Solid purple symbols correspond to FRET experiments where VEGFR2 was labeled with YFP, and transparent purple symbols correspond to FRET experiments where EGFR was labeled with YFP (364 data points total). (D) Effect of 56 nM VEGF on EGFR-VEGFR2 hetero-FRET. Solid pink symbols correspond to FRET experiments where VEGFR2 was labeled with YFP, and transparent pink symbols correspond to FRET experiments where EGFR was labeled with YFP (370 data points total). (E) Expressions measured in all heterodimer experiments, shown as the concentration of VEGFR2 *versus* EGFR.

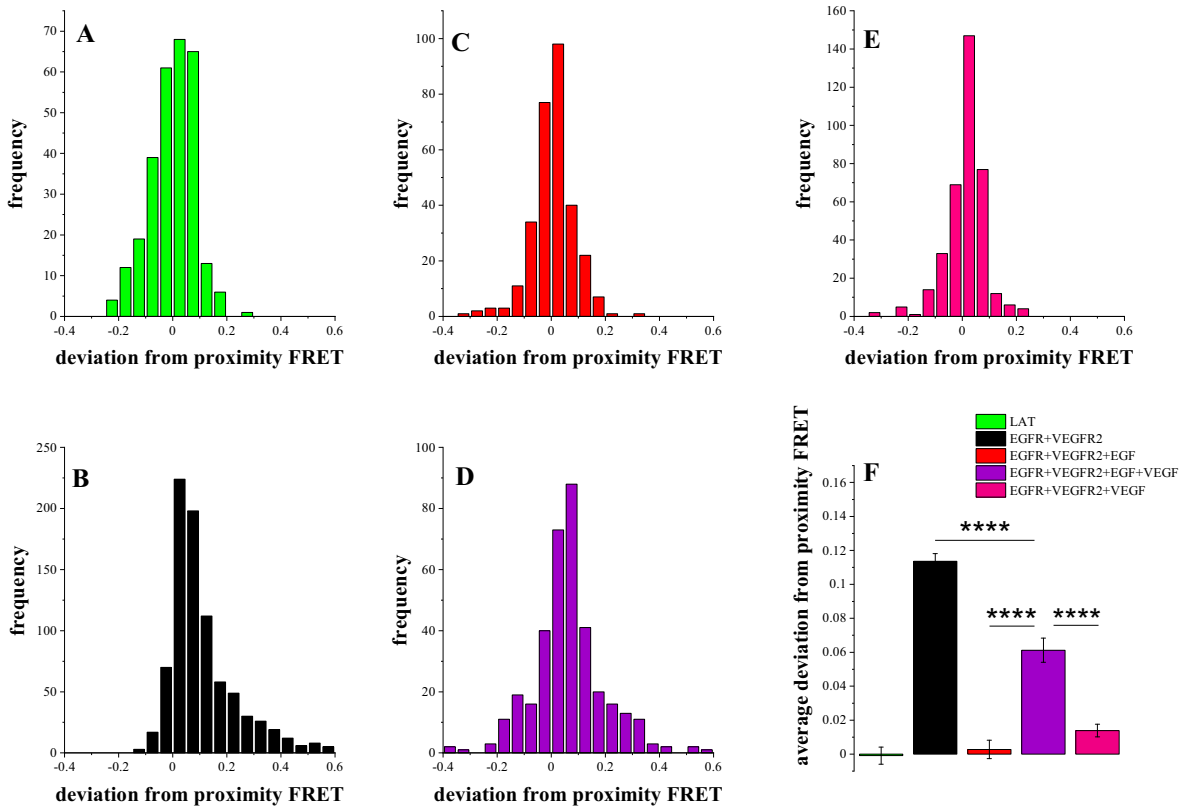

Figure 3. Deviations from proximity FRET. Data from individual cells expressing either (A) LAT or (B–E) both ECTM EGFR and ECTM VEGFR2 in the absence of ligand (B), the presence of 10 nM EGF (C), 10 nM EGF and 56 nM VEGF (D), or 56 nM VEGF (E). (F) Average deviations from proximity FRET and standard errors. The average deviation from proximity FRET is −0.0009 ± 0.005 for LAT,[29] 0.1136 ± 0.0045 for EGFR and VEGFR2 in the absence of ligand,[29] 0.003 ± 0.005 in the presence of EGF only,[29] 0.061 ± 0.007 in the presence of EGF and VEGF, and 0.014 ± 0.004 in the presence of VEGF only. Differences between LAT, EGFR + VEGFR2 + EGF, and EGFR + VEGFR2 + VEGF are not statistically significant. Differences between EGFR + VEGFR2 + EGF + VEGF, and VEGFR2 + VEGFR + EGF/EGFR + VEGFR + VEGF are highly statistically significant ($p < 0.0001$, ****), based on one way ANOVA.

transition model views unliganded and liganded RTKs as structurally distinct signaling entities.[15]

Based on the current knowledge about RTK signaling, the observed heterointeractions in our experiments probably involve EGF-bound EGFR dimers and VEGF-bound VEGFR2 dimers, as at high ligand concentrations both EGFR and VEGFR2 exist as ligand-bound dimers.[19,56,57] It is likely that the ligand-bound EGFR and VEGFR2 dimers interact laterally to form higher-order oligomers, giving rise to FRET in Figure 2(C). Such oligomers have not been described thus far in the RTK literature, to the best of our knowledge. However, oligomerization in response to ligand binding has been implicated in important signaling responses. For instance, EGFR has been proposed to form oligomers in addition to dimers, and the ligand-bound oligomers are believed to be more active than the ligand-bound dimers. Specifically, it has been suggested that the phosphorylation of the proximal tyrosines in the C-terminal tail is more efficient in the EGFR oligomers than in the EGFR dimers.[39,58] By being part of a larger complex, each kinase may be able to both phosphorylate other tyrosines and be phosphorylated, leading to higher over-all RTK phosphorylation, as well as to higher phosphorylation of downstream effectors.[39,58] Thus, homooligomerization may be a mechanism that allows for signal amplification and/or diversification. It is possible that a similar phenomenon occurs in the putative EGFR-VEGFR2 heterooligomers, and its role may be to further amplify and/or diversity signaling outputs. Furthermore, it is possible that heterooligomerization is not exclusive for the EGFR-VEGFR2 pair, but can occur for many RTKs. Indeed, the literature contains many examples of complex signaling processes occurring when multiple RTKs and multiple cognate ligands are present.[24]

It is known that RTK signaling can lead to different biological outcomes in different cellular contexts, though mechanisms that are poorly understood.[24,59–62] This work hints at a novel mechanism through which different cellular contexts can

specify signaling, namely through the regulation of co-expression of different receptors and their cognate ligands. The differential expression, in turn, will control the formation of different heterocomplexes of ligand-bound RTK dimers. These heterocomplexes could exhibit different signaling properties, as compared to homodimers and homooligomers. The importance of this mechanism in cell signaling is yet to be investigated, and so are its biological consequences and therapeutic potential.

CRediT authorship contribution statement

Michael D. Paul: Conceptualization, Investigation, Visualization, Writing - original draft. **Kalina Hristova:** Conceptualization, Funding acquisition, Supervision, Visualization, Writing - review & editing.

Acknowledgements

Supported by NIH GM068619. We thank Elmer Zapata-Mercado for technical help and Dr. Marek Cebecauer for providing us with the LAT plasmid used to construct LAT-MT and LAT-eYFP.

Declaration of Competing Interest

The authors declare that they have no known competing financial interests or personal relationships that could have appeared to influence the work reported in this paper.

Received 11 January 2021;
Accepted 15 April 2021;
Available online 20 April 2021

Keywords:
receptor tyrosine kinases;
EGFR;
VEGFR2;
heterooligomers;
cell signaling

References

1. Lemmon, M.A., Schlessinger, J., (2010). Cell signaling by receptor tyrosine kinases. *Cell*, **141**, 1117–1134.
2. Trenker, R., Jura, N., (2020). Receptor tyrosine kinase activation: From the ligand perspective. *Curr. Opin. Cell Biol.*, **63**, 174–185.
3. Schlessinger, J., (2002). Ligand-induced, receptor-mediated dimerization and activation of EGF receptor. *Cell*, **110**, 669–672.
4. Pasquale, E.B., (2010). Eph receptors and ephrins in cancer: bidirectional signalling and beyond. *Nature Rev. Cancer*, **10**, 165–180.
5. Li, E., Hristova, K., (2006). Role of receptor tyrosine kinase transmembrane domains in cell signaling and human pathologies. *Biochemistry*, **45**, 6241–6251.
6. He, L., Hristova, K., (2012). Physical-chemical principles underlying RTK activation, and their implications for human disease. *BBA*, **1818**, 995–1005.
7. Schlessinger, J., (2014). Receptor tyrosine kinases: legacy of the first two decades. *Cold Spring Harb. Perspect. Biol.*, **6**
8. Sergina, N.V., Moasser, M.M., (2007). The HER family and cancer: emerging molecular mechanisms and therapeutic targets. *Trends Mol. Med.*, **13**, 527–534.
9. Browne, B.C., O'Brien, N., Duffy, M.J., Crown, J., O'Donovan, N., (2009). HER-2 signaling and inhibition in breast cancer. *Curr. Cancer Drug Targets*, **9**, 419–438.
10. Noberini, R., Lamberto, I., Pasquale, E.B., (2012). Targeting Eph receptors with peptides and small molecules: progress and challenges. *Semin. Cell Dev. Biol.*, **23**, 51–57.
11. Cochet, C., Kashles, O., Chambaz, E.M., Borrello, I., King, C.R., Schlessinger, J., (1988). Demonstration of epidermal growth factor-induced receptor dimerization in living cells using a chemical covalent cross-linking agent. *J. Biol. Chem.*, **263**, 3290–3295.
12. Lemmon, M.A., Schlessinger, J., (1994). Regulation of signal-transduction and signal diversity by receptor oligomerization. *TIBS*, **19**, 459–463.
13. Bocharov, E.V., Mineev, K.S., Pavlov, K.V., Akimov, S.A., Kuznetsov, A.S., Efremov, R.G., Arseniev, A.S., (2017). Helix-helix interactions in membrane domains of bitopic proteins: specificity and role of lipid environment. *Biochim. Biophys. Acta, Mol. Cell. Biol. Lipids*, **1859**, 561–576.
14. Purba, E.R., Saita, E.I., Maruyama, I.N., (2017). Activation of the EGF receptor by ligand binding and oncogenic mutations: the "rotation model". *Cells*, **6**
15. Paul, M.D., Hristova, K., (2019). The transition model of RTK activation: A quantitative framework for understanding RTK signaling and RTK modulator activity. *Cytokine Growth Factor Rev.*, **49**, 23–31.
16. Moriki, T., Maruyama, H., Maruyama, I.N., (2001). Activation of preformed EGF receptor dimers by ligand-induced rotation of the transmembrane domain. *J. Mol. Biol.*, **311**, 1011–1026.
17. Valley, C.C., Lewis, A.K., Sachs, J.N., (2017). Piecing it together: Unraveling the elusive structure-function relationship in single-pass membrane receptors. *Biochim. Biophys. Acta, Mol. Cell. Biol. Lipids*, **1859**, 1398–1416.
18. Sarabipour, S., Hristova, K., (2016). Mechanism of FGF receptor dimerization and activation. *Nature Commun.*, **7**, 10262.
19. Sarabipour, S., Ballmer-Hofer, K., Hristova, K., (2016). VEGFR-2 conformational switch in response to ligand binding. *Elife*, **5**
20. Hyde, C.A., Giese, A., Stuttfeld, E., Abram, S.J., Villemagne, D., Schleier, T., Binz, H.K., Ballmer-Hofer, K., (2012). Targeting extracellular domains D4 and D7 of vascular endothelial growth factor receptor 2 reveals allosteric receptor regulatory sites. *Mol. Cell. Biol.*, **32**, 3802–3813.
21. Doerner, A., Scheck, R., Schepartz, A., (2015). Growth factor identity is encoded by discrete coiled-coil rotamers in the EGFR Juxtamembrane Region. *Chem. Biol.*, **22**, 776–784.
22. Ahmed, F., Hristova, K., (2018). Dimerization of the Trk receptors in the plasma membrane: effects of their cognate ligands. *Biochem. J.*, **457**, 3669–3685.

23. Lin, C.C., Melo, F.A., Ghosh, R., Suen, K.M., Stagg, L.J., Kirkpatrick, J., Arold, S.T., Ahmed, Z., et al., (2012). Inhibition of basal FGF receptor signaling by dimeric Grb2. *Cell*, **149**, 1514–1524.
24. Paul, M.D., Hristova, K., (2019). The RTK interactome: overview and perspective on RTK heterointeractions. *Chem. Rev.*, **119**, 5881–5921.
25. Grausporta, D., Beerli, R.R., Daly, J.M., Hynes, N.E., (1997). ErbB-2, the preferred heterodimerization partner of all ErbB receptors, is a mediator of lateral signaling. *EMBO J.*, **16**, 1647–1655.
26. Alimandi, M., Romano, A., Curia, M.C., Muraro, R., Fedi, P., Aaronson, S.A., Difiore, P.P., Kraus, M.H., (1995). Cooperative signaling of Erbb3 and Erbb2 in neoplastic transformation and human mammary carcinomas. *Oncogene*, **10**, 1813–1821.
27. Olayioye, M.A., Neve, R.M., Lane, H.A., Hynes, N.E., (2000). The ErbB signaling network: receptor heterodimerization in development and cancer. *EMBO J.*, **19**, 3159–3167.
28. Del Piccolo, N., Sarabipour, S., Hristova, K., (2017). A new method to study heterodimerization of membrane proteins and its application to fibroblast growth factor receptors. *J. Biol. Chem.*, **292**, 1288–1301.
29. Paul, M.D., Grubb, H.N., Hristova, K., (2020). Quantifying the strength of heterointeractions among receptor tyrosine kinases from different subfamilies: Implications for cell signaling. *J. Biol. Chem.*, **295**, 9917–9933.
30. Yokote, H., Fujita, K., Jing, X., Sawada, T., Liang, S., Yao, L., Yan, X., Zhang, Y., et al., (2005). Trans-activation of EphA4 and FGF receptors mediated by direct interactions between their cytoplasmic domains. *Proc. Natl. Acad. Sci. USA*, **102**, 18866–18871.
31. Yamaguchi, T., Yanagisawa, K., Sugiyama, R., Hosono, Y., Shimada, Y., Arima, C., Kato, S., Tomida, S., Suzuki, M., Osada, H., Takahashi, T., (2012). NKX2-1/TITF1/TTF-1-Induced ROR1 is required to sustain EGFR survival signaling in lung adenocarcinoma. *Cancer Cell*, **21**, 348–361.
32. Li, C., Wang, S., Xing, Z., Lin, A., Liang, K., Song, J., Hu, Q., Yao, J., et al., (2017). A ROR1-HER3-lncRNA signalling axis modulates the Hippo-YAP pathway to regulate bone metastasis. *Nature Cell Biol.*, **19**, 106–119.
33. Festuccia, C., Gravina, G.L., Muzi, P., Millimaggi, D., Dolo, V., Vicentini, C., Ficorella, C., Ricevuto, E., et al., (2009). Her2 crosstalks with TrkA in a subset of prostate cancer cells: rationale for a guided dual treatment. *Prostate*, **69**, 337–345.
34. Choy, C., Ansari, K.I., Neman, J., Hsu, S., Duenas, M.J., Li, H., Vaidehi, N., Jandial, R., (2017). Cooperation of neurotrophin receptor TrkB and Her2 in breast cancer cells facilitates brain metastases. *Breast Cancer Res.*, **19**, 51.
35. Lu, K.V., Chang, J.P., Parachoniak, C.A., Pandika, M.M., Aghi, M.K., Meyronet, D., Isachenko, N., Fouse, S.D., et al., (2012). VEGF inhibits tumor cell invasion and mesenchymal transition through a MET/VEGFR2 complex. *Cancer Cell*, **22**, 21–35.
36. Greenberg, J.I., Shields, D.J., Barillas, S.G., Acevedo, L.M., Murphy, E., Huang, J., Scheppke, L., Stockmann, C., et al., (2008). A role for VEGF as a negative regulator of pericyte function and vessel maturation. *Nature*, **456**, 809–813.
37. Cheng, C., Haasdijk, R.A., Tempel, D., den Dekker, W.K., Chrifi, I., Blonden, L.A., van de Kamp, E.H., de Boer, M., et al., (2012). PDGF-induced migration of vascular smooth muscle cells is inhibited by heme oxygenase-1 via VEGFR2 upregulation and subsequent assembly of inactive VEGFR2/PDGFRbeta heterodimers. *Arterioscler. Thromb. Vasc. Biol.*, **32**, 1289–1298.
38. Needham, S.R., Roberts, S.K., Arkhipov, A., Mysore, V.P., Tynan, C.J., Zanetti-Domingues, L.C., Kim, E.T., Losasso, V., et al., (2016). EGFR oligomerization organizes kinase-active dimers into competent signalling platforms. *Nature Commun.*, **7**, 13307.
39. Huang, Y., Bharill, S., Karandur, D., Peterson, S.M., Marita, M., Shi, X., Kaliszewski, M.J., Smith, A.W., et al., (2016). Molecular basis for multimerization in the activation of the epidermal growth factor receptor. *Elife*, **5**
40. Stein, E., Lane, A.A., Cerretti, D.P., Schoecklmann, H.O., Schroff, A.D., Van Etten, R.L., Daniel, T.O., (1998). Eph receptors discriminate specific ligand oligomers to determine alternative signaling complexes, attachment, and assembly responses. *Genes Dev.*, **12**, 667–678.
41. Chen, J., Hicks, D., Brantley-Sieders, D., Cheng, N., McCollum, G.W., Qi-Werdich, X., Penn, J., (2006). Inhibition of retinal neovascularization by soluble EphA2 receptor. *Exp. Eye Res.*, **82**, 664–673.
42. Hess, A.R., Margaryan, N.V., Seftor, E.A., Hendrix, M.J., (2007). Deciphering the signaling events that promote melanoma tumor cell vasculogenic mimicry and their link to embryonic vasculogenesis: role of the Eph receptors. *Develop. Dyn.: Off. Publ. Am. Assoc. Anatomists*, **236**, 3283–3296.
43. Baharuddin, W.N.A., Yusoff, A.A.M., Abdullah, J.M., Osman, Z.F., Ahmad, F., (2018). Roles of EphA2 receptor in angiogenesis signaling pathway of glioblastoma multiforme. *The Malaysian J. Med. Sci: MJMS*, **25**, 22.
44. Amin, D.N., Bielenberg, D.R., Lifshits, E., Heymach, J.V., Klagsbrun, M., (2008). Targeting EGFR activity in blood vessels is sufficient to inhibit tumor growth and is accompanied by an increase in VEGFR-2 dependence in tumor endothelial cells. *Microvasc. Res.*, **76**, 15–22.
45. Naumov, G.N., Nilsson, M.B., Cascone, T., Briggs, A., Straume, O., Akslen, L.A., Lifshits, E., Byers, L.A., Xu, L., Wu, H.-K., (2009). Combined vascular endothelial growth factor receptor and epidermal growth factor receptor (EGFR) blockade inhibits tumor growth in xenograft models of EGFR inhibitor resistance. *Clin. Cancer Res.*, **15**, 3484–3494.
46. Cascone, T., Herynk, M.H., Xu, L., Du, Z., Kadara, H., Nilsson, M.B., Oborn, C.J., Park, Y.-Y., Erez, B., Jacoby, J. J., (2011). Upregulated stromal EGFR and vascular remodeling in mouse xenograft models of angiogenesis inhibitor–resistant human lung adenocarcinoma. *J. Clin. Investig.*, **121**, 1313–1328.
47. King, C., Stoneman, M., Raicu, V., Hristova, K., (2016). Fully quantified spectral imaging reveals in vivo membrane protein interactions. *Integr. Biol. (Camb.)*, **8**, 216–229.
48. Biener, G., Stoneman, M.R., Acbas, G., Holz, J.D., Orlova, M., Komarova, L., Kuchin, S., Raicu, V., (2014). Development and experimental testing of an optical micro-spectroscopic technique incorporating true line-scan excitation. *Int. J. Mol. Sci.*, **15**, 261–276.
49. King, C., Sarabipour, S., Byrne, P., Leahy, D.J., Hristova, K., (2014). The FRET signatures of noninteracting proteins in membranes: simulations and experiments. *Biophys. J.*, **106**, 1309–1317.

50. King, C., Raicu, V., Hristova, K., (2017). Understanding the FRET signatures of interacting membrane proteins. *J. Biol. Chem.*, **292**, 5291–5310.
51. Macdonald, J.L., Pike, L.J., (2008). Heterogeneity in EGF-binding affinities arises from negative cooperativity in an aggregating system. *PNAS*, **105**, 112–117.
52. Terman, B.I., Dougher-Vermazen, M., Carrion, M.E., Dimitrov, D., Armellino, D.C., Gospodarowicz, D., Bohlen, P., (1992). Identification of the KDR tyrosine kinase as a receptor for vascular endothelial cell growth factor. *Biochem. Biophys. Res. Commun.*, **187**, 1579–1586.
53. Waltenberger, J., Claessonwelsh, L., Siegbahn, A., Shibuya, M., Heldin, C.H., (1994). Different signal-transduction properties of Kdr and Flt 1, 2 receptors for vascular endothelial growth-factor. *J. Biol. Chem.*, **269**, 26988–26995.
54. Kilpatrick, L.E., Friedman-Ohana, R., Alcobia, D.C., Riching, K., Peach, C.J., Wheal, A.J., Briddon, S.J., Robers, M.B., Zimmerman, K., Machleidt, T., Wood, K.V., Woolard, J., Hill, S.J., (2017). Real-time analysis of the binding of fluorescent VEGF165a to VEGFR2 in living cells: Effect of receptor tyrosine kinase inhibitors and fate of internalized agonist-receptor complexes. *Biochem. Pharmacol.*, **136**, 62–75.
55. Peach, C.J., Kilpatrick, L.E., Friedman-Ohana, R., Zimmerman, K., Robers, M.B., Wood, K.V., Woolard, J., Hill, S.J., (2018). Real-time ligand binding of fluorescent VEGF-A isoforms that discriminate between VEGFR2 and NRP1 in living cells. *Cell Chem. Biol.*, **25** 1208–1218 e1205.
56. Singh, D.R., King, C., Salotto, M., Hristova, K., (2019). Revisiting a controversy: The effect of EGF on EGFR dimer stability. *Biochim. Biophys. Acta, Biomembr.*,.
57. Chung, I., Akita, R., Vandlen, R., Toomre, D., Schlessinger, J., Mellman, I., (2010). Spatial control of EGF receptor activation by reversible dimerization on living cells. *Nature*, **464**, 783–U163.
58. Needham, S.R., Roberts, S.K., Arkhipov, A., Mysore, V.P., Tynan, C.J., Zanetti-Domingues, L.C., Kim, E.T., Losasso, V., et al., (2016). EGFR oligomerization organizes kinase-active dimers into competent signalling platforms. *Nature Commun.*, **7**
59. Speth, Z., Islam, T., Banerjee, K., Resat, H., (2017). EGFR signaling pathways are wired differently in normal 184A1L5 human mammary epithelial and MDA-MB-231 breast cancer cells. *J Cell Commun Signal*, **11**, 341–356.
60. Adachi, K., Nikaido, I., Ohta, H., Ohtsuka, S., Ura, H., Kadota, M., Wakayama, T., Ueda, H.R., et al., (2013). Context-dependent wiring of Sox2 regulatory networks for self-renewal of embryonic and trophoblast stem cells. *Mol. Cell*, **52**, 380–392.
61. Nandi, S., Gutin, G., Blackwood, C.A., Kamatkar, N.G., Lee, K.W., Fishell, G., Wang, F., Goldfarb, M., et al., (2017). FGF-dependent, context-driven role for FRS adapters in the early telencephalon. *J. Neurosci.*, **37**, 5690–5698.
62. Karl, K., Paul, M.D., Pasquale, E.B., Hristova, K., (2020). Ligand bias in receptor tyrosine kinase signaling. *J. Biol. Chem.*, **295**, 18494–18507.
63. Adamkova, L., Kvicalova, Z., Rozbesky, D., Kukacka, Z., Adamek, D., Cebecauer, M., Novak, P., (2019). Oligomeric architecture of mouse activating Nkrp1 receptors on living cells. *Int. J. Mol. Sci.*, **20**
64. Ahmed, F., Zapata-Mercado, E., Rahman, S., Hristova, K., (2021). The biased ligands NGF and NT-3 differentially stabilize Trk-A dimers. *Biophys. J.*, **120**, 55–63.
65. Ahmed, F., Paul, M.D., Hristova, K., (2020). The biophysical basis of receptor tyrosine kinase ligand functional selectivity: Trk-B case study. *Biochem. J.*, **477**, 4515–4526.